



HAL
open science

3D Architecture of Human Lower Leg Muscles assessed with Ultra High-Field Diffusion Tensor Imaging and Tractography: Sensitivity to Sex-Difference and Intramuscular Variability

Alexandre Fouré, Augustin C. Ogier, Arnaud Le Troter, Thorsten Feiweier, Christophe Vilmen, Maxime Guye, Julien Gondin, Pierre Besson, Bendahan David

► **To cite this version:**

Alexandre Fouré, Augustin C. Ogier, Arnaud Le Troter, Thorsten Feiweier, Christophe Vilmen, et al.. 3D Architecture of Human Lower Leg Muscles assessed with Ultra High-Field Diffusion Tensor Imaging and Tractography: Sensitivity to Sex-Difference and Intramuscular Variability. *Imaging in Neuromuscular Disease (Myo-MRI 2017)*, Nov 2017, Berlin, Germany. hal-04077634

HAL Id: hal-04077634

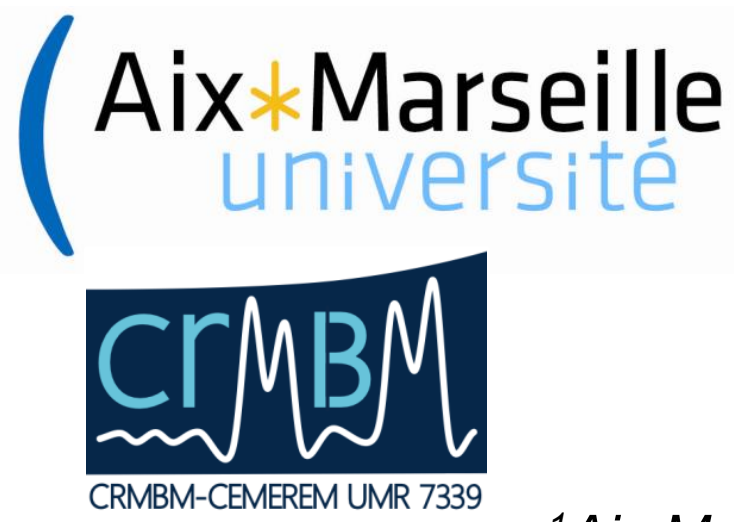
<https://hal.science/hal-04077634>

Submitted on 24 Apr 2023

HAL is a multi-disciplinary open access archive for the deposit and dissemination of scientific research documents, whether they are published or not. The documents may come from teaching and research institutions in France or abroad, or from public or private research centers.

L'archive ouverte pluridisciplinaire **HAL**, est destinée au dépôt et à la diffusion de documents scientifiques de niveau recherche, publiés ou non, émanant des établissements d'enseignement et de recherche français ou étrangers, des laboratoires publics ou privés.

3D ARCHITECTURE OF HUMAN LOWER LEG MUSCLES ASSESSED WITH ULTRA-HIGH-FIELD DIFFUSION TENSOR IMAGING AND TRACTOGRAPHY: SENSITIVITY TO SEX DIFFERENCE AND INTRAMUSCULAR VARIABILITY



Fouré A¹, Ogier A¹, Le Troter A¹, Feiweier T⁴, Vilmen C¹,
Guye M^{1,2}, Gondin J^{1,3}, Besson P¹, Bendahan D¹



¹Aix Marseille Univ, CNRS, CRMBM, Marseille, France

²APHM, Hôpitaux de la Timone, CEMEREM, Marseille, France

³Université Claude Bernard, Institut NeuroMyoGène, UMR CNRS 5310 – INSERM U1217, Villeurbanne, France

⁴Siemens Healthcare, Erlangen, Allemagne

Introduction

Neuromuscular disorders induce skeletal muscle function impairments related to changes in both **muscle volume** and **structural arrangement of fascicles/fibers** within the muscle leading to the reduction of skeletal muscle force production [1]. However, the estimation of both muscle volume and architecture in a single experimental session remains challenging.

Although ultrasonography remains the gold standard to assess muscle architecture, a method based on the **diffusion tensor imaging (DTI)** and **fiber tractography** allows a **3D characterization of architecture** in the whole muscular volume [2]. It was demonstrated that higher is the signal-to-noise ratio and better are the tractography results [3]. Thus, **ultra-high-field MRI** appears of utmost interest and relevance to accurately assess skeletal muscle diffusion tensor parameters and 3D architecture.

The aim of the study was to demonstrate the sensitivity of the lower leg muscles 3D structural organization measurements using DTI assessed with ultra-high-field (7T) MRI and tractography of lower leg skeletal muscles fibers. **Sex difference and intramuscular variability** previously reported in superficial muscles with ultrasonography [4] were determined.

Materials & Methods

Experimental population. Twenty young healthy subjects (10 men: 22 ± 3 y, 174 ± 5 cm, 66 ± 7 kg and 10 women: 23 ± 3 y, 165 ± 8 cm, 57 ± 7 kg) volunteered to participate.

MRI explorations. Subjects were positioned supine in a 7T MAGNETOM whole body research scanner (Siemens Medical System, Erlangen). Lower leg muscles were explored with a 28-channel proton knee coil. The foot was maintained at ~20° in plantar flexion (0°: foot perpendicular to the tibia). Muscles volume was quantified from T₁-weighted images (120 slices, FOV = 180 × 180 mm²; matrix = 384 × 384; acquisition time = 8 min 34 s).

Axial multidirectional diffusion weighted images (DWI) were acquired with a standard “monopolar” Stejskal-Tanner diffusion encoding scheme – *i.e.*, a single spin-echo refocusing. A standard chemically-selective fat suppression was used and a gradient-reversal technique has been added to improve the saturation efficiency. Data were acquired in two opposite phase-encoding polarities to correct for distortions with the following parameters: 120 slices, FOV = 180 mm × 180 mm²; matrix = 120 × 120; slice thickness = 1,5 mm; 30 directions; b values = 0 et 500 s/mm²; acquisition time = 7 min 54 s.

Muscle segmentation. Regions of interest were manually drawn on T₁-weighted images using FSLview software (Fig.1). Muscle areas were segmented every 5 slices, and missing slices were automatically interpolated [5]. Muscle volume was calculated by summing the volume of each muscle in all the slices.

Corrections of DWI. Each diffusion-weighted dataset was denoised using BM4D algorithm. Geometric and signal distortions were estimated on b = 0 s/mm² images with the *topup* function from FSL software and modifications were applied to correct images from these distortions and Eddy currents using FSL *eddy* function.

Intensity of non-distorted diffusion- and T₁-weighted images were corrected from B₁ homogeneities using N4ITK algorithm from *ants* library. Finally, each T₁-weighted image was registered with the image obtained for b = 0 s/mm² using 3D rigid-body transformation, subsequently applied to muscle segmentation masks.

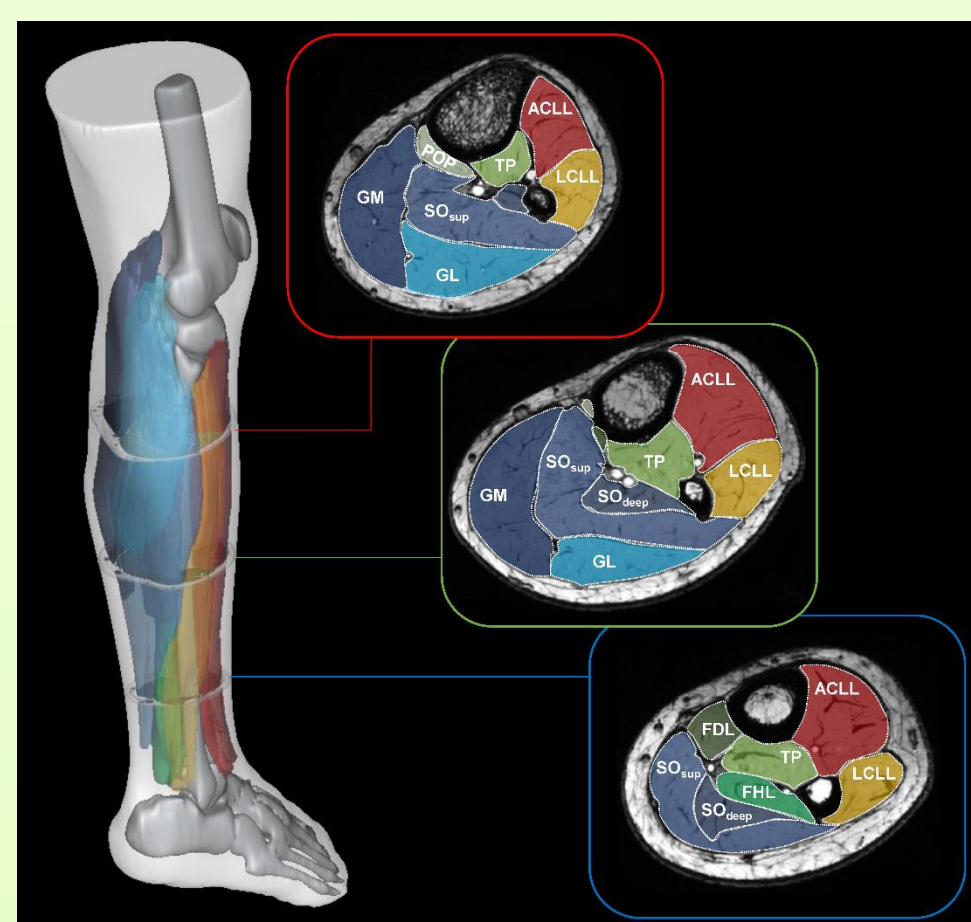


Fig.1 : Segmentation of the lower leg muscles

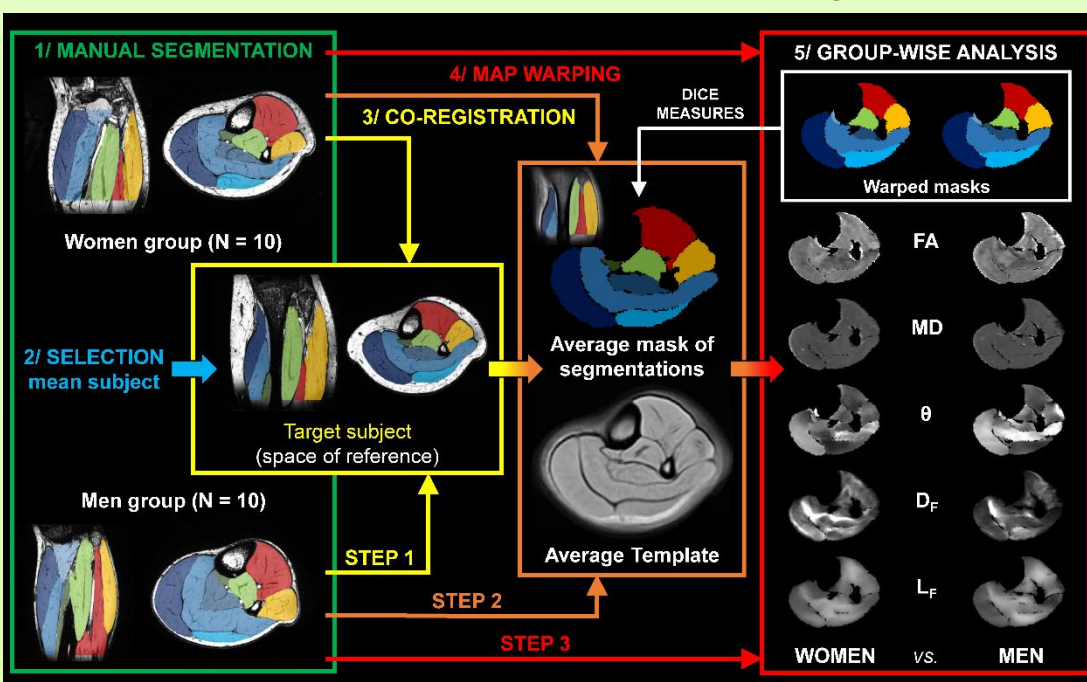


Fig.2 : Pipeline of data processing for the 3D spatial normalization

3D muscle architecture.

From muscle fiber tractography, muscle fiber length (L_F) and pennation angle (θ) were characterized. θ was determined as the angle between the muscle's principal axis and the global direction of each fiber tracked within the muscle. L_F and θ were averaged over all fiber tracts within each voxel.

Statistical analysis.

A 3D spatial normalization and statistical parametric mapping (SPM) were performed on the basis of an original methodology (Fig.2) previously described [6]. Muscle volume was then divided in three equal parts (*i.e.*, distal, central and proximal) to discriminate potential change in architecture parameters along muscle and across sex.

Results

Significant sex differences were detected in muscle volume (+ 21.7 % in men for the entire lower leg, $P = 0.008$).

Significant sex differences were found in fiber length of all DPCLL muscles (*i.e.*, L_F men > L_F women for FHL, FDL, TP and POP) and pennation angle of FDL but SPM analysis revealed only few significant local differences regarding to sex.

Differences were found independently of sex in architecture along several muscles of the lower leg (Fig.3).

For instance, L_F was significantly higher in the central part for GL, FHL and POP but lower in the distal part for GM, SO_{sup}, FHL, LCLL and ACLL. θ was lower in proximal part of SO_{sup}, TP and ACLL

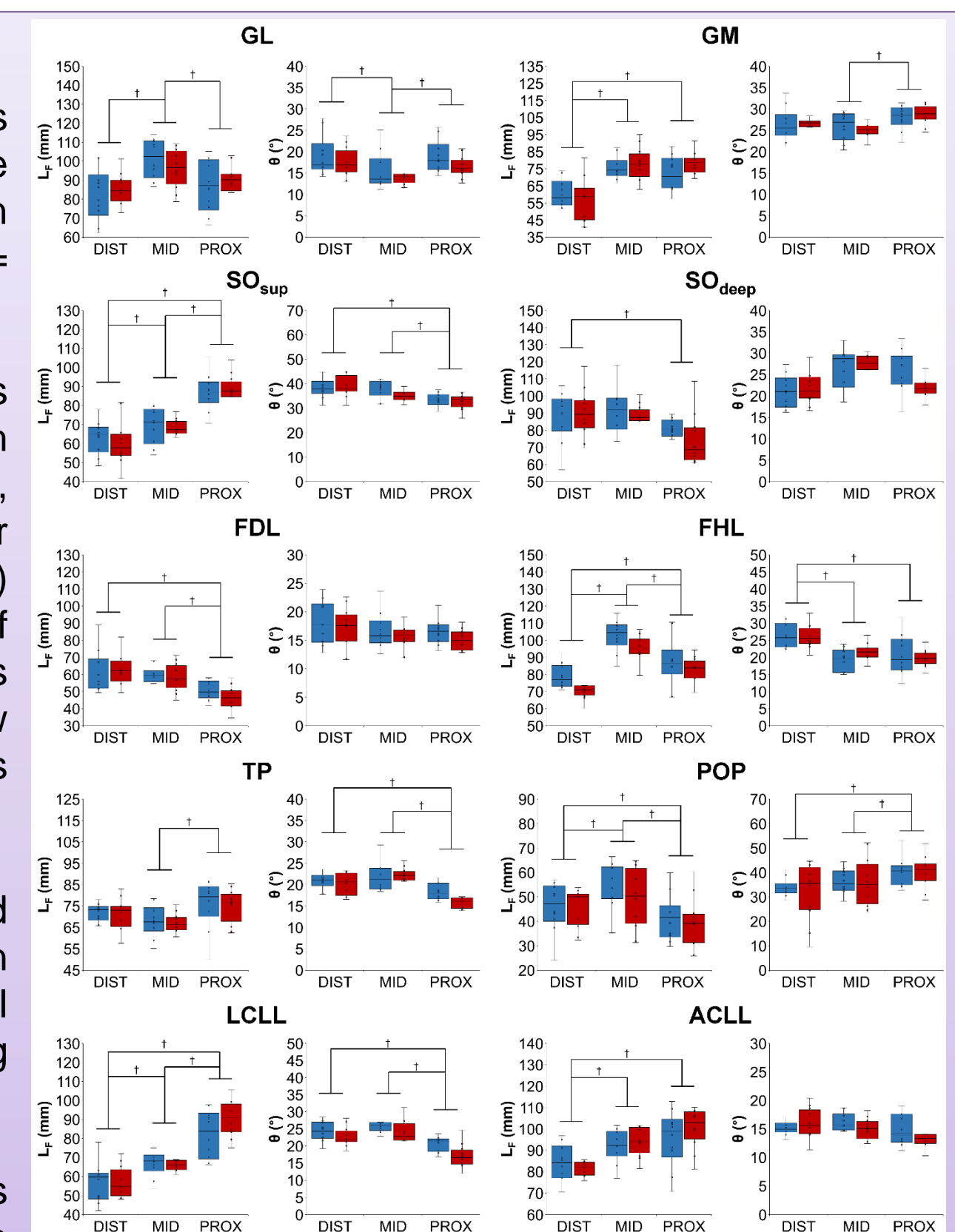


Fig.3: Fiber length (L_F) and pennation angle (θ) in the distal (DIST), central (MID) and proximal (PROX) parts of the lower leg muscles in men (blue) and women (red). L_F and θ was altered along muscles (gastrocnemius medialis [GM], gastrocnemius lateralis [GL], soleus [SO], flexor hallucis longus [FHL], flexor digitorum longus [FDL], tibialis posterior [TP], popliteus [POP] and muscles included in the lateral [LCLL] and anterior [ACLL] compartment of the lower leg).

*: significant difference between parts and sex (post-hoc comparison from length × sex interaction effect). †: significant difference between parts (post-hoc comparison from length main effect).

Conclusion

3D muscle architecture assessed from diffusion tensor imaging with ultra-high-field MRI and tractography are sensitive to sex but only slight differences were detected in lower leg muscles fiber length and pennation angle of young healthy populations. The combination of diffusion tensor imaging-derived parametric maps 3D coregistration and statistical parametric mapping analysis shed light on additional differences along lower leg muscles in both sexes.

Assessment at once and on a large spatial coverage of all the lower leg muscle volume, diffusion properties and 3D architecture with 7T-MRI provides reproducible parameters that might help in diagnostic of muscle tissue alterations leading to muscle function impairments.

Bibliography

- [1] Lieber RL, Friden J. Clinical significance of skeletal muscle architecture. Clin Orthop Relat Res. 2001(383):140-51.
- [2] Heemskerk AM, Sinha TK, Wilson KJ, Ding Z, Damon BM. Quantitative assessment of DTI-based muscle fiber tracking and optimal tracking parameters. Magn Reson Med. 2009;61(2):467-72.
- [3] Damon BM. Effects of image noise in muscle diffusion tensor (DT)-MRI assessed using numerical simulations. Magn Reson Med. 2008;60(4):934-44.
- [4] Chow RS, Medri MK, Martin DC, Leekam RN, Agur AM, McKee NH. Sonographic studies of human soleus and gastrocnemius muscle architecture: gender variability. Eur J Appl Physiol. 2000;82(3):236-44.
- [5] Ogier A, Sdika M, Fouré A, Le Troter A, Bendahan D. Individual muscle segmentation in MR Images: a 3D propagation through 2D non-linear registration approaches. 39th Annual International Conference of the IEEE Engineering in Medicine and Biology Society (EMBC'17). 2017:317-20.
- [6] Fouré A, Le Troter A, Guye M, Mattei JP, Bendahan D, Gondin J. Localization and quantification of intramuscular damage using statistical parametric mapping and skeletal muscle parcellation. Sci Rep. 2015 5:18580.

This study was supported by the following grants: Equipex 7T-AMI ANR-11-EQPX-0001, A*MIDEX-EI-13-07-130115-08.38-7TAMISTART, A*MIDEX ANR-11-IDEX-0001-02.

The authors thank the Assistance Publique des Hôpitaux de Marseille (APHM), the Centre National de la Recherche Scientifique (CNRS UMR 7339) and all the volunteers involved in this study.

alexandre.foure@hotmail.fr

alexandre.foure@univ-amu.fr